

You Share Beliefs, I Adapt: Progressive Heterogeneous Collaborative Perception

Hao Si Ehsan Javanmardi Manabu Tsukada *

The University of Tokyo

{si-hao, ejavanmardi, mtsukada}@g.ecc.u-tokyo.ac.jp

Abstract

Collaborative perception enables vehicles to overcome individual perception limitations by sharing information, allowing them to see further and through occlusions. In real-world scenarios, models on different vehicles are often heterogeneous due to manufacturer variations. Existing methods for heterogeneous collaborative perception address this challenge by fine-tuning adapters or the entire network to bridge the domain gap. However, these methods are impractical in real-world applications, as each new collaborator must undergo joint training with the ego vehicle on a dataset before inference, or the ego vehicle stores models for all potential collaborators in advance. Therefore, we pose a new question: Can we tackle this challenge directly during inference, eliminating the need for joint training? To answer this, we introduce Progressive Heterogeneous Collaborative Perception (PHCP), a novel framework that formulates the problem as few-shot unsupervised domain adaptation. Unlike previous work, PHCP dynamically aligns features by self-training an adapter during inference, eliminating the need for labeled data and joint training. Extensive experiments on the OPV2V dataset demonstrate that PHCP achieves strong performance across diverse heterogeneous scenarios. Notably, PHCP achieves performance comparable to SOTA methods trained on the entire dataset while using only a small amount of unlabeled data. Code is available at: <https://github.com/sihaool/PHCP>

1. Introduction

Recent advances in Vehicle-to-Everything (V2X) have improved the capability of autonomous driving systems[12, 40, 42]. V2X enables vehicles to interact with the surrounding environment, creating a more intelligent and interconnected traffic ecosystem. With the support of V2X, Collaborative Perception allows vehicles to share perception information[22, 24, 31], thus expanding the range of perception and empowering the ability to see through occlusion[9].

*Corresponding author

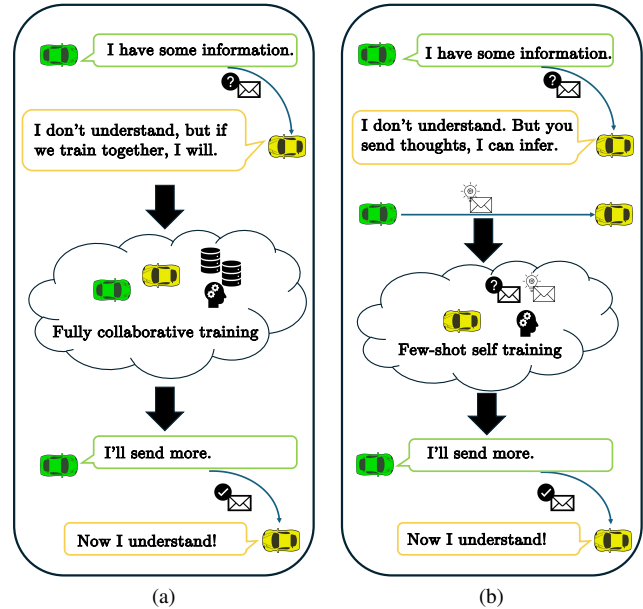


Figure 1. Illustration of different heterogeneous collaborative perception patterns. Fig. 1a corresponds to existing methods requiring joint training before collaboration. Fig. 1b shows our PHCP process. It utilizes a small amount of unlabeled data from other agents to complete self-training and collaborate with others.

This achieves a more precise and robust environmental perception in complex urban traffic environments.

Despite the potential of collaborative perception in improving the performance of autonomous driving systems, it faces a major challenge in the real world: heterogeneity[14, 19–21, 36, 39]. Autonomous vehicles produced by different manufacturers typically adopt different sensor configurations and perception models, resulting in significant differences in the encoded intermediate features in the semantic space (domain gap)[36]. This problem makes collaborative perception between intelligent agents difficult and may lead to ineffective information sharing and feature fusion.

Many existing methods enhance heterogeneous collaborative perception by training feature encoders and detection heads[19, 36] or by learning adapters[20] for new collabo-

rators. While these approaches improve performance, they remain limited in their generalization to newly added agents. As shown in Fig. 1a, this limitation implies that whenever a new agent joins the collaboration, the model or adapter must be trained, and additional parameters must be stored. However, with the continuous emergence of new sensors and perception models, it becomes impractical for autonomous vehicles to maintain dedicated adapters or models for every potential collaborator. This highlights the need for a more flexible and scalable heterogeneous collaborative perception framework. To address this challenge, we propose a new question: **Can the ego vehicle dynamically change its model parameters during the inference stage for different collaborators without relying on joint training or any prior knowledge of them?**

Solving this problem presents several key challenges: (1) Lack of supervision in the inference stage. Unlike the training stage, the inference process lacks additional annotations. Therefore, a core challenge is leveraging unsupervised learning methods to fine-tune the model and achieve feature alignment. (2) Constraints on data volume and computational time. Given the real-time requirements of collaborative perception, we aim to minimize both the training data amount and fine-tune iterations after the collaboration relationship is confirmed.

To address these challenges, we propose a Progressive Heterogeneous Collaborative Perception (PHCP) framework based on self-training and few-shot unsupervised domain adaptation. This framework aligns features in semantic space by only a small amount of unlabeled data from collaborating agents in the inference stage. The overall workflow consists of two stages. In stage I, the agent generates pseudo labels from its predictions and transmits them with intermediate features to the ego vehicle. Upon receiving this information, the ego vehicle fine-tunes an adapter by a few-shot learning approach. In stage II, the agent transmits only the intermediate features, while the ego vehicle uses the well-trained adapter to transform the features and then perform fusion and prediction. We conduct extensive experiments on the OPV2V dataset, and the results demonstrate that our method outperforms the direct collaboration baseline by approximately 30% in heterogeneous collaborative perception scenarios. Our main contributions are summarized as follows:

- To the best of our knowledge, this is the first work to tackle the domain gap in heterogeneous collaborative perception during the inference process.
- We provide a new perspective to address this challenge through few-shot unsupervised domain adaptation. We propose a novel collaborative perception scheme and framework, generating effective supervision labels during inference and enabling the ego vehicle to fine-tune the adapter and resolve the domain gap issues within a

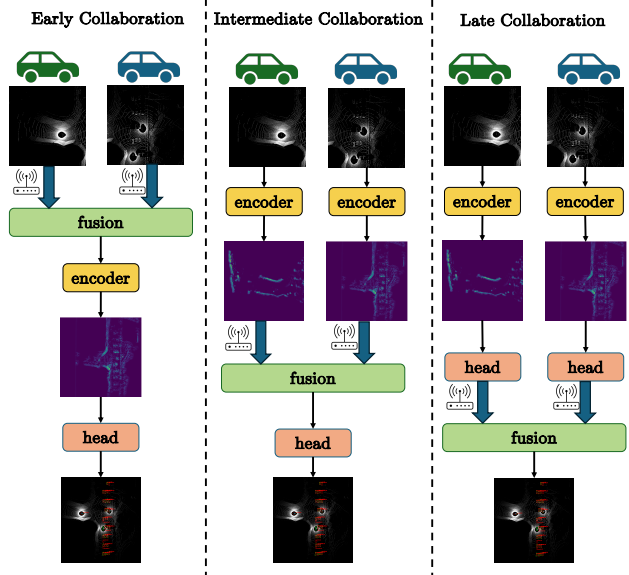


Figure 2. Comparison of different collaborative perception schemes.

few iterations,

- We conducted extensive experiments across various scenarios, demonstrating the robustness of our method in heterogeneous collaborative perception.

2. Related Work

Collaborative perception. Collaborative perception improves perception performance by fusing shared information among connected vehicles. As shown in the Fig. 2, collaborative perception can be categorized into early, late, and intermediate collaboration depending on the type of shared data[9]. In early collaboration, raw sensor data such as LiDAR point clouds and RGB images are directly fused at the data level after calibration and spatial alignment, resulting in a more comprehensive environmental perception[1, 4, 8]. Although this method performs well, the transmission of large amounts of raw data from the vehicle poses challenges to the V2X network. In late collaboration, object-level fusion is used, where agents only share perception results. After post-processing steps like spatial transformation and non-maximum suppression, the final detection results are generated[2, 7, 23, 41]. This method is simple to implement and has low bandwidth requirements but is more sensitive to noise and localization errors, leading to relatively lower performance. Intermediate collaboration is a feature-level fusion, gaining increasing attention in recent years. It transmits feature-level data while sharing and preserving semantic information, effectively reducing data transmission volume[10, 17, 26]. It's a trade-

off solution between early and late collaboration. Recent studies[5, 11, 15, 16, 18, 25, 38] have focused on this scheme. F-Cooper[3] is the pioneering work in this field, introducing a low-level voxel fusion approach and a spatial feature fusion strategy. V2VNet[27] leverages graph neural networks to model agent communication, achieving a balance between accuracy and bandwidth requirements. AttFusion[35] introduces a single-head self-attention fusion module to capture spatial relationships within feature maps. CoBEVT[33] explores an alternative approach by replacing LiDAR with cameras, proposing a fused axial attention module that effectively integrates camera-based BEV features, enhancing perception performance in a LiDAR-free scenario. However, these methods assume that all agents share the same model and parameters[19, 20, 36], which is unrealistic in the real world. So, recent studies have shifted their focus toward heterogeneous collaborative perception, aiming to address this challenge.

Heterogeneous Collaborative perception. V2X-ViT[34] was the first to address the heterogeneity problem. It treats vehicle-to-infrastructure and vehicle-to-vehicle as two fusion types and proposes the Heterogeneous Multi-Agent Attention module to perform fusion among heterogeneous agents. HM-ViT[30] extends heterogeneous collaborative perception to multi-sensor settings, introducing a heterogeneous 3D graph attention module that effectively fuses BEV features from different modalities. MPDA[36] focuses on model-level heterogeneity and employs a learnable feature resizer to align features, along with a sparse cross-domain transformer to bridge the domain gap. PnPDA[20] introduces a novel plug-and-play domain adapter, effectively bridging the domain gap without destructing the models. HEAL[19] proposes a new framework that establishes a unified feature space for all agents, ensuring that when a new agent joins the collaboration, it only needs to be aligned to this shared space rather than adapting to every collaborator. Although these methods address the domain gap caused by heterogeneity, they rely on prior training on the dataset and lack the flexibility to adapt to newly introduced agents.

3. Method

In this paper, we explore achieving progressive collaboration in heterogeneous scenarios without relying on joint training or prior knowledge of other agents. Our method first generates pseudo labels from agents to facilitate self-training for the ego. This process is completed within a very limited number of frames. Subsequently, the agent only needs to share intermediate features, while the ego performs feature fusion and final prediction, thereby enhancing collaboration efficiency and addressing the domain gap problem. Fig.3 illustrates the main workflow.

3.1. Problem Formulation

The collaborative perception at the feature level can be divided into two stages. In the first stage, all agents use their own encoders to process the raw data and generate feature maps, which are then shared. In the second stage, ego vehicles perform fusion on all agents’ features, and then the detection head is used to predict the results. Consider N agents in the scene, where χ_i represents the i th agent. The process can be described as follows:

$$\mathbf{F}_i = \text{enc}_i(d_i), \quad \mathbf{F}_i \in \mathcal{S} \quad (1)$$

$$\mathbf{P}_i = \text{head}_i(\text{fuse}_i(\mathbf{F}_1, \mathbf{F}_2, \dots, \mathbf{F}_n)) \quad (2)$$

where d_i denotes χ_i ’s original data, P_i is the final prediction result. enc_i is feature encoder of χ_i , which outputs the feature map F_i . The feature fusion module fuse_i is responsible for spatial-temporal alignment and feature integration. head_i is the classification head for χ_i , predicting the target position and confidence score based on the feature map. If heterogeneity is considered, the intermediate features F_i generated by the encoding may belong to different semantic spaces. To address this, we can use feature adapters to map the features of different agents to the ego’s feature space.

$$\mathbf{F}'_i = \Phi_{i \rightarrow \text{ego}}(\mathbf{F}_i), \quad \mathbf{F}'_i \in \mathcal{S}_{\text{ego}}, \mathbf{F}_i \in \mathcal{S}_i \quad (3)$$

Our target is to address the heterogeneity problem by achieving adaptive adjustment of the adapter $\Phi_{i \rightarrow \text{ego}}()$ during the collaborative perception inference stage with only a small amount of unlabeled data.

3.2. Feature Adapter

Our approach employs a feature adapter to bridge the domain gap between the source \mathcal{S}_i and target domains \mathcal{S}_{ego} . Since we perform training on a small dataset, the adapter structure must remain simple to prevent overfitting. Through visual analysis of feature maps in Fig.4, we observed that while the overall feature distributions of the source and target domains are similar, they show misalignment in channel dimensions and certain critical regions. We found CBAM[29] to be particularly well-suited for this task. CBAM effectively addresses this issue by incorporating both channel and spatial attention mechanisms. The channel attention module(CAM) directs the network to focus on important channels, while the spatial attention module(SAM) enhances attention to crucial spatial regions. CBAM’s lightweight design also introduces minimal computational overhead, making it an efficient and practical choice for our method.

3.3. PHCP Scheme

We adopt a novel collaborative perception approach between intermediate and late collaboration, ensuring the generation of pseudo-labeled data without introducing excessive communication overhead. Specifically, after establishing the

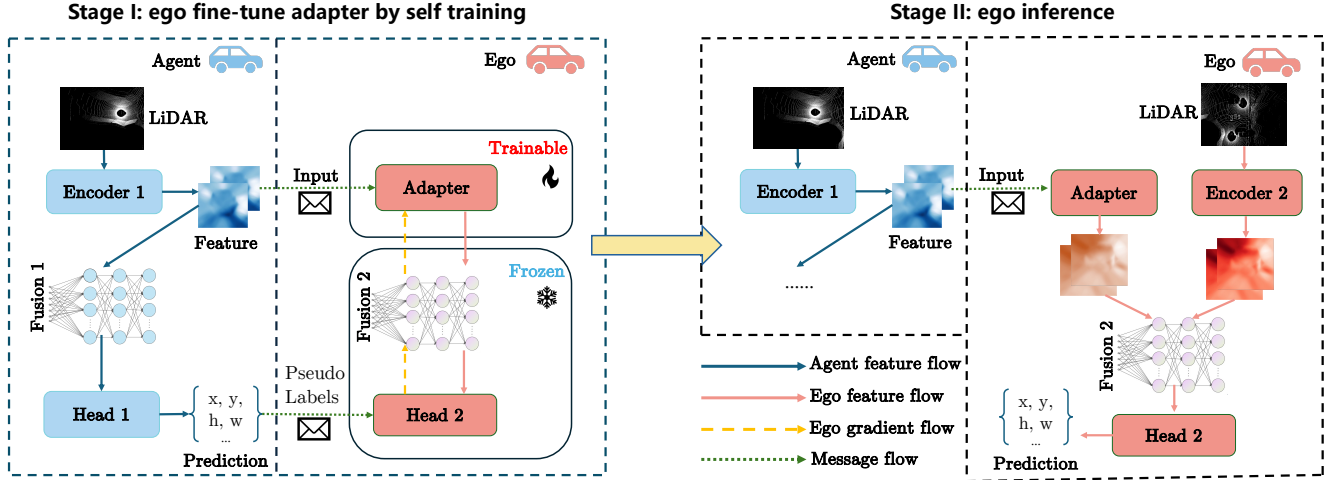


Figure 3. Overview of our proposed heterogeneous collaboration process. In Stage I, the ego performs self-training using pseudo labels to fine-tune the adapter. In Stage II, the ego applies the adapter to transform features and then perform fusion and prediction.

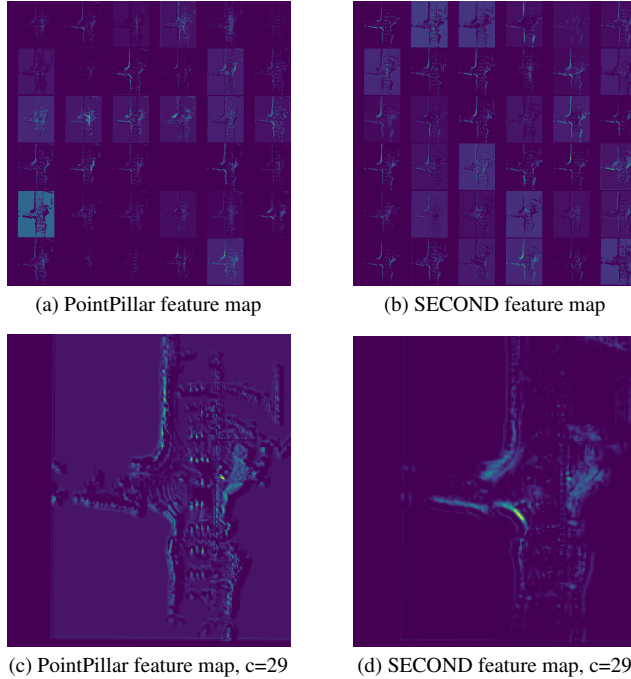


Figure 4. **Illustration of domain gap of different encoders.** We visualized the encoder’s output features by displaying each channel’s absolute values. Figure 4a and Figure 4b illustrate the misalignment in the channel dimension. Figures 4c and 4d explain the differences in the area of interest

collaboration relationship, in the first k frames, the agent simultaneously sends features and detection results to the ego, and the ego uses this information to update the feature adapter. We define this as the stage I. The updated method will be introduced later. After k frames, the collaboration

process follows the normal intermediate collaboration process, with the agent only sending features to the ego. This corresponds to stage II. We determine the value of k by referring to typical values in few-shot learning, choosing 1, 5, or 10.

3.4. PHCP Process

This progressive collaboration process consists of two stages. In the first stage, the ego trains its own adapter using features and pseudo-labels provided by agents through a few-shot self-training way. In the second stage, the ego aligns the features of the agents by the adapter and then performs fusion and prediction.

Stage I. We aim to optimize the ego’s adapter without prior knowledge about agents in this stage. Due to the lack of labels, we use agents’ predictions as pseudo-labels. In particular, we select high-quality predictions as pseudo-labels based on confidence scores, and we also record the corresponding confidence scores as soft labels instead of one-hot labels. In this way, we can create dataset $\mathcal{D}_i = \{(d_1, p_1), \dots, (d_k, p_k) \mid d \in \mathcal{S}_i\}$ as a small training sample dataset (the support set). Our model optimization strategy builds upon a two-stage fine-tuning approach (TFA)[28] due to its simplicity and efficiency. We introduce further enhancements to improve its adaptability within our collaborative perception framework. Considering that the detectors of ego and agent have already been trained separately before the collaboration begins, we only need to focus on the second fine-tuning stage. In the second stage, we fix all the parameters of the fusion network and the detector head and only fine-tune the adapters. This is because the ego needs to use the same fusion network and detector head for different agents. When collaborating with multiple agents

Algorithm 1 Stage I: adapter fine-tuning

```
1: for each scenario do
2:   Input:  $\{F_i\}, \mathbf{F}_i = \{d_1, \dots, d_k\}$   $\triangleright$  shared feature
   from each agent
3:   for each agent  $\chi_i$  except ego do
4:      $\mathcal{H}_i = \{F_j \mid \chi_j \text{ is homogeneous to } \chi_i\}$   $\triangleright$ 
   aggregate all agents that are homogeneous to the current
5:      $\mathbf{P}_i = \text{head}_i(\text{fuse}_i(\mathcal{H}))$ 
6:      $\mathcal{D}_i = \{\mathcal{H}_i, \mathbf{P}_i\}$ 
7:   end for
8:   for each agent  $\chi_i$  except ego do
9:      $\mathbf{L}_i, \mathcal{H}_i \leftarrow \mathcal{D}_i$ 
10:     $\mathbf{P}_i = \text{head}_{ego}(\text{fuse}_{ego}(\mathcal{H}_i))$ 
11:     $\Phi_{i \rightarrow ego} \leftarrow \nabla \text{Loss}(\mathbf{L}_i, \mathbf{P}_i)$ 
12:   end for
13:   Output:  $\Phi_{i \rightarrow ego}$   $\triangleright$  feature adapters from agents to
   ego
14: end for
```

simultaneously, fine-tuning the model on multiple datasets may introduce mutual interference, reducing its adaptability to each agent and degrading overall performance. However, the adapter is created independently by the ego for each agent, and by only adjusting the adapter, isolation can be achieved, and interference can be reduced. In the fine-tuning process, we adopt a scheduler with a warm-up mechanism. We select one scenario for hyperparameter tuning, while the remaining scenarios are for testing. We train a total of 20 rounds, and due to the small training data size, the overall computational overhead is very low.

Stage II. This stage follows immediately after the first stage. We consider the features shared by agents as the query set $\mathcal{Q}_i = \{d_{k+1}, \dots, d_N \mid d \in \mathcal{S}_i\}$. We believe that after the training in the first stage, the adapter can effectively address the domain gap problem. Subsequently, the transformed features \mathcal{Q}'_i and the features from the ego's encoder can be fused to obtain the final detection results. We use the aver-

Algorithm 2 Stage II: Inference

```
1: for each scenario do
2:   Input:  $\{F_i\}, \mathbf{F}_i = d_{k+1}, \dots, d_N$   $\triangleright$  shared feature
   from each agent
3:   for each agent  $\chi_i$  except ego do
4:      $F'_i = \Phi_{i \rightarrow ego}(F_i)$ 
5:      $\mathcal{F}_i = F_i \cup F'_i$ 
6:   end for
7:    $\mathbf{P}_{ego} = \text{head}_{ego}(\text{fuse}_{ego}(\mathcal{F}_i))$ 
8:   Output:  $\mathbf{P}_{ego}$   $\triangleright$  ego final prediction
9: end for
```

age AP value of all scenarios as the final evaluation metric,

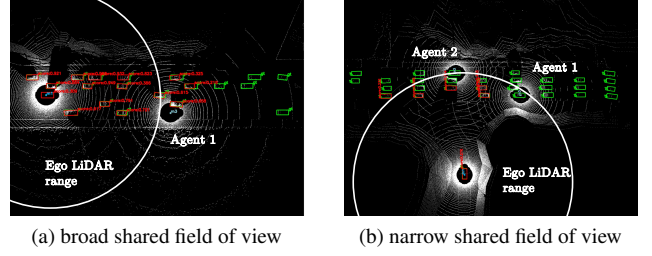


Figure 5. Detection performance under different ego vehicle field of view conditions

referred to as mean scenario AP (mSAP). This is because we observe significant differences in the data distribution among different scenarios. In Fig.5a, most of the objects are concentrated on one side of the ego vehicle, and even without receiving information from other agents, the final detection results are not affected. However, in Fig.5b, the objects are mainly distributed on the side of agent vehicles. If the ego vehicle cannot effectively utilize the feature information from agents, it may result in many false negatives. Therefore, mSAP, as a comprehensive performance evaluation metric, can more fairly measure the detection capability of the model in different scenarios.

4. Experiments

4.1. Datasets and Evaluation

We use OPV2V[35] and its supplementary dataset, OPV2V-H[19] as the dataset for model training and evaluation. OPV2V is collected by the simulation tools OpenCDA[32] and CARLA[6], covering various complex driving scenarios, including challenging situations such as severe occlusion. We use the default dataset splitting ratio. The training and validation sets are used to train the baseline model for homogeneous collaborative perception, and the test set is used to evaluate the performance of heterogeneous collaborative perception. We further divide the test dataset according to the scenario settings, resulting in 16 specific scenarios. For each scenario, we split them into support sets \mathcal{S} and query sets \mathcal{Q} , and the sizes are determined by the number of shots. We adopt mSAP at Intersection-over-Union (IoU) thresholds of 0.3, 0.5, and 0.7 to evaluate the model performance.

4.2. Experimental Setups

We adopt two types of agents with different LiDAR encoders: agent LP using the PointPillars[13] encoder and agent LS using the SECOND[37] module. Feature fusion is performed using the multi-scale pyramid fusion method proposed by HEAL[19]. The overall training and validation procedure of the model is as follows: on the OPV2V dataset, we conducted homogeneous collaborative perception training for LP and LS respectively using two RTX 6000ADA GPUs, so

Method	AP@IoU 0.5 in Scenarios																mSAP@IoU		
	1	2	3	4	5	6	7	8	9	10	11	12	13	14	15	16	0.3	0.5	0.7 ↑
Direct Fusion	83.2	31.9	68.2	69.0	83.9	54.7	54.3	86.8	59.9	35.0	40.2	40.5	34.0	55.4	82.0	72.5	59.7	59.5	53.0
PHCP(Ours)	96.2	98.4	96.2	94.2	96.3	95.2	82.6	97.0	95.2	95.9	88.9	96.2	80.6	85.6	90.9	89.0	92.9	92.4	85.9

Table 1. Comparison between our methods and the direct fusion baseline

Method	AP@IoU 0.7 in Scenarios																mSAP@IoU		
	1	2	3	4	5	6	7	8	9	10	11	12	13	14	15	16	0.3	0.5	0.7 ↑
F-Cooper[3]	84.1	50.8	69.7	56.3	79.4	65.5	57.0	76.1	61.2	57.6	58.0	60.9	48.4	49.6	72.6	77.3	91.2	83.1	63.4
CoBEVT[33]	78.7	67.2	79.5	71.8	82.0	71.2	62.2	87.4	70.3	71.2	66.4	60.4	54.1	66.8	83.9	79.7	94.8	91.2	72.0
AttFusion[35]	84.0	68.5	87.0	71.4	92.6	78.6	63.7	84.0	72.8	73.5	74.4	76.3	65.1	75.7	83.7	84.9	93.0	89.9	77.3
V2X-ViT[34]	81.7	74.9	90.8	79.2	88.7	84.8	65.7	92.1	90.1	81.3	78.4	87.6	73.1	83.4	90.6	82.6	94.3	92.3	82.8
PHCP(Ours)	89.2	92.6	90.4	87.4	92.2	94.1	67.1	95.2	89.6	94.7	84.7	91.5	70.7	83.8	89.0	80.8	92.8	92.3	87.1
HEAL[19]	89.1	93.4	97.6	91.3	93.6	96.6	76.2	97.2	93.0	97.5	89.7	94.5	86.9	87.7	93.1	90.0	95.5	95.1	91.7

Table 2. Comparison between PHCP and other methods. Notably, we achieve these results using only a small amount of unlabeled data.

we get base models $\mathcal{M}_{LP} = \{Enc_{LP}, Fuse_{LP}, Head_{LP}\}$ and $\mathcal{M}_{LS} = \{Enc_{LS}, Fuse_{LS}, Head_{LS}\}$. Subsequently, on the dataset \mathcal{S} , we extract intermediate features by Enc_{LS} and generate prediction results using model $Head_{LS}$ as pseudo-labels. Then, we perform fine-tuning on the sub-model $\{\Phi()_{LS \rightarrow LP}, Fuse_{LP}, Head_{LP}\}$ with this pseudo-labeled data. Only the adapter is trainable, while the parameters of other modules are fixed. Finally, we combine the adapter with M_{LP} to form a new model $\mathcal{M}'_{LP} = \{Enc_{LP}, \Phi()_{LS \rightarrow LP}, Fuse_{LP}, Head_{LP}\}$, and then evaluated it on the dataset \mathcal{Q} .

Optimization Strategy. We employ a scheduler that combines the warmup and multi-step decay strategies. In the warmup stage, we use a linear strategy, where the warmup factor was set to 0.001, and the warmup lasted for 8 epochs. During the actual training process, the learning rate decayed at the 12th and 16th epochs with a decay factor of 0.1. Our base learning rate was set to 0.005, the batch size was set to 1, and the training was completed within 20 epochs.

Comparison. Our direct fusion baseline method uses models LS and LP, which have not undergone joint training, for direct collaborative perception. This setting aligns with real-world heterogeneous collaboration, as we have no prior knowledge of each other’s model structures or parameters before collaboration begins. Additionally, we compare our approach with other collaborative perception methods, which were fine-tuned on the training dataset before testing. For models that do not support heterogeneous collaborative perception, such as F-Cooper[3], V2X-ViT[34], AttFusion[35], and CoBEVT[33], we first train the models in homogeneous scenarios and then perform 40 fine-tuning epochs in heterogeneous scenarios. For models that support heterogeneous collaborative perception, like HEAL[19], we follow the training methods provided by the authors.

4.3. Quantitative evaluation

Main performance comparison. Tab.1 presents a comparison between our method and the direct fusion baseline across various scenarios. Our method consistently outperforms the baseline by 33.2%, 32.9%, and 32.9% in AP@0.3, AP@0.5, and AP@0.7. Our method still achieves strong results even in some challenging scenarios where the baseline performs poorly. Tab.2 further compares our approach with other collaborative perception methods. Except for HEAL, which achieves the SOTA performance, our method surpasses all others. It is important to note that while other methods utilize the full training dataset with labels, our approach achieves comparable performance using only a minimal amount of unlabeled data.

Computational cost. As detailed in Tab.3, the training phase takes between 1.5 and 2.4 seconds depending on the number of shots. The inference takes 0.07 seconds. Importantly, the few-shot training process is executed only once when a new collaborative relationship is established. So the overall computational cost meets the real-time requirements.

Stage	Setting	Time(s)	Mem(MB)
Training	shots=1, bs=1	1.49	1290
	shots=2, bs=2	1.71	2314
	shots=4, bs=4	2.17	4552
	shots=5, bs=5	2.39	5604
Inference	-	0.07	798

Table 3. Computation cost of training and inference. All training configurations use 20 iterations; **shots** indicates the number of shots used for training, and **bs** is the batch size.

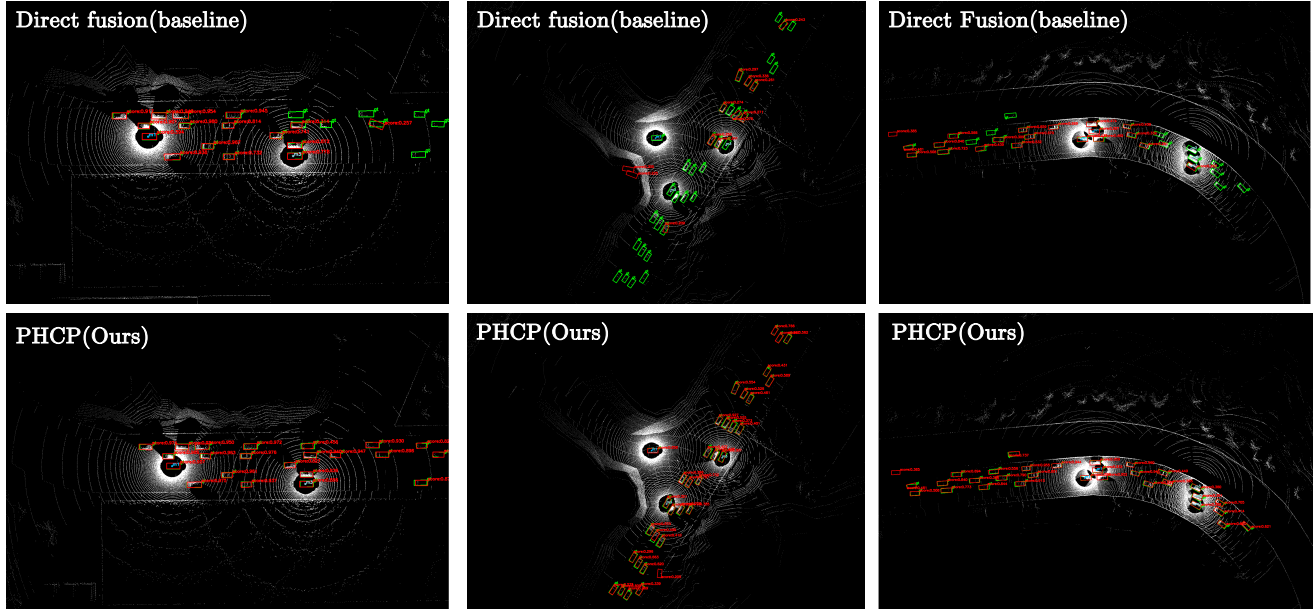


Figure 6. Visual comparison of three scenarios between our method and the baseline. Each scenario involves two, three, and four collaborative agents participating in collaborative perception. The red and green boxes represent the prediction and ground truth.

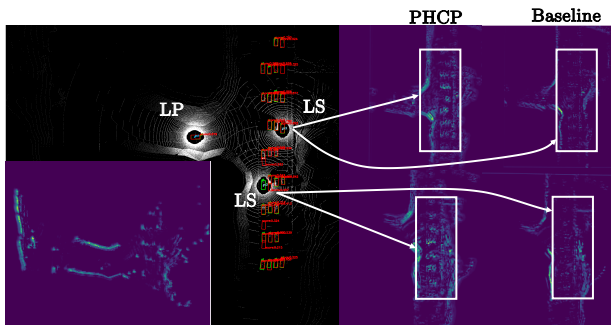


Figure 7. Feature map visualization comparison between our method and baseline

4.4. Qualitative results

Visualization of detection results. Fig. 6 presents the qualitative visualizations of our method and the baseline. We select three scenarios with varying numbers of collaborative agents. Due to the lack of effective feature fusion, the baseline method has many false negatives outside the ego vehicle’s field of view. In contrast, our approach successfully detects these objects.

Visualization of feature map. Fig. 7 shows a collaborative scenario involving three agents. By comparing the feature maps, we observe that our method achieves more effective feature alignment with the ego vehicle than the baseline.

4.5. Ablation studies

Trade-off between performance and number of shots. A larger number of shots represents more training data, which usually leads to more accurate prediction results. However, it also increases the waiting time for initiating collaboration. Therefore, we analyze the relation between the number of shots and model performance. In our experiments, 0-shot means direct collaboration and serves as the baseline. Fig. 8 illustrates the relation between the number of shots and the model’s performance. Even when relying only on single-frame data, our model still achieves a performance improvement of approximately 50%. As the number of shots increases, the AP@IoU 0.7 also improves. This suggests that more training data can better optimize the adapter module, enhance the quality of fused feature maps, and thus achieve more precise localization and higher prediction accuracy.

Quality of the pseudo label. The quality of pseudo labels impacts the final performance. We evaluate the pseudo labels on the test set and obtained an AP@0.5 of 0.86 and an AP@0.7 of 0.78; 80% of the predictions have confidence scores greater than 0.5. Then we conduct an analysis of different filtering strategies. We set a series of confidence thresholds to filter pseudo-labels or directly used the confidence scores as soft labels. We evaluate the performance using mSAP and AP in the worst-case scenarios (wSAP) for a comprehensive comparison. From Tab. 4, retaining only high-quality pseudo labels results in insufficient positive samples, limiting the model’s learning capacity. Conversely, low-quality pseudo labels introduce noise, leading to a de-

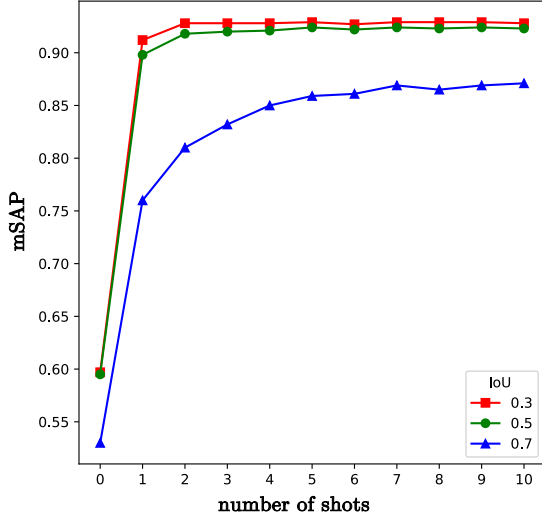


Figure 8. Performance of different number of shots

cline in overall model accuracy. However, the impact of pseudo-label quality on the final results remains relatively minor. We attribute this to the spatial attention mechanism in the adapter, which effectively focuses on target regions.

	0.2	0.5	0.7	soft
mSAP@0.7	85.0	85.9	85.8	85.4
wSAP@0.7	66.1	68.0	67.7	67.0

Table 4. Performance under different pseudo label confidence levels

Comparison between heterogeneous and homogeneous settings. From Tab.5, while our baseline model performs well under homogeneous conditions, its performance drops when applied directly to heterogeneous scenarios. This contrast highlights that even strong homogeneous collaboration models cannot effectively handle heterogeneity. In contrast, our method effectively addresses this challenge and maintain robust performance in heterogeneous settings.

Method	mSAP@IoU		
	0.3	0.5	0.7
Direct Fusion(baseline)	59.7	59.5	53.0
PHCP	92.9	92.4	85.9
SECOND (homogeneous)	94.8	94.2	90.5
PointPillar (homogeneous)	96.2	95.8	93.1

Table 5. Heterogeneous vs. homogeneous collaborative perception.

Generalization across scenarios. In this study, we conduct separate training and testing on each scenario because each

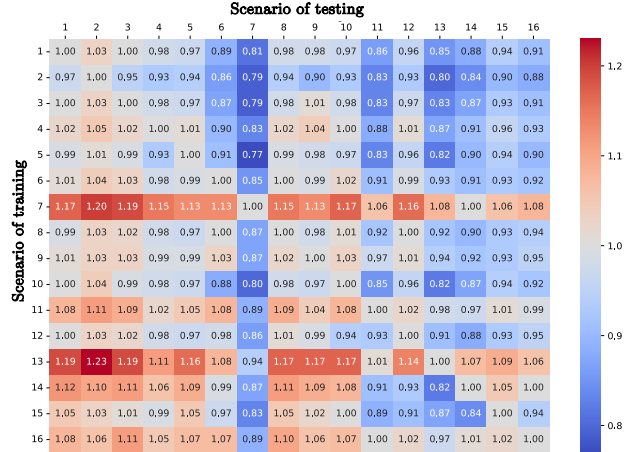


Figure 9. Cross-scenario evaluation results. The figure presents test results across different scenarios. The values have been normalized using the diagonal elements. The overall generalization performance is strong except for a few particularly challenging scenarios where all models perform poorly.

scenario corresponds to a new collaborative relationship, and our model validation aims to assess its adaptability in each new heterogeneous collaboration environment. We also performed cross-scenario testing to verify the model’s generalization ability and ensure it does not overfit a single scenario. Specifically, we train a base model for each scenario and used its AP@IoU 0.5 inference results as a baseline. Then, without any additional fine-tuning, we directly test the same model on other scenarios to analyze its generalization ability in different environments. The results in Fig.9 indicate that although the model’s performance slightly declines in some complex scenarios, it remains stable in most scenarios. This result further validates the adaptability and generalization of our model.

5. Conclusion

We introduce PHCP, a novel heterogeneous collaborative perception framework designed to address feature misalignment during the inference stage of collaborative perception, where training on a dataset with collaborators is unrealistic, and collaborators’ prior knowledge is unavailable. The key idea is to utilize pseudo labels generated by other agents and perform few-shot self-training on the ego vehicle to fine-tune the adapter module, thereby bridging the domain gap between the ego and agents. Extensive experiments on the OPV2V dataset demonstrate the effectiveness of our approach, outperforming baseline methods across various heterogeneous collaborative perception scenarios. Compared to other methods trained on the entire dataset, our approach achieves performance comparable to SOTA methods while using only a small amount of unlabeled data.

Acknowledgments

This work was supported by JST, CRONOS, Japan Grant Number JPMJCS24K8.

References

- [1] Eduardo Arnold, Mehrdad Dianati, Robert de Temple, and Saber Fallah. Cooperative perception for 3d object detection in driving scenarios using infrastructure sensors. *IEEE Transactions on Intelligent Transportation Systems*, 23(3): 1852–1864, 2020. 2
- [2] Dian Chen and Philipp Krähenbühl. Learning from all vehicles. In *Proceedings of the IEEE/CVF Conference on Computer Vision and Pattern Recognition*, pages 17222–17231, 2022. 2
- [3] Qi Chen, Xu Ma, Sihai Tang, Jingda Guo, Qing Yang, and Song Fu. F-cooper: Feature based cooperative perception for autonomous vehicle edge computing system using 3d point clouds. In *Proceedings of the 4th ACM/IEEE Symposium on Edge Computing*, pages 88–100, 2019. 3, 6
- [4] Qi Chen, Sihai Tang, Qing Yang, and Song Fu. Cooper: Cooperative perception for connected autonomous vehicles based on 3d point clouds. In *2019 IEEE 39th International Conference on Distributed Computing Systems (ICDCS)*, pages 514–524. IEEE, 2019. 2
- [5] Jiaxun Cui, Hang Qiu, Dian Chen, Peter Stone, and Yuke Zhu. Coopernaut: End-to-end driving with cooperative perception for networked vehicles. In *Proceedings of the IEEE/CVF Conference on Computer Vision and Pattern Recognition*, pages 17252–17262, 2022. 3
- [6] Alexey Dosovitskiy, German Ros, Felipe Codevilla, Antonio Lopez, and Vladlen Koltun. Carla: An open urban driving simulator. In *Conference on robot learning*, pages 1–16. PMLR, 2017. 5
- [7] Chen Fu, Chiyu Dong, Christoph Mertz, and John M Dolan. Depth completion via inductive fusion of planar lidar and monocular camera. In *2020 IEEE/RSJ International Conference on Intelligent Robots and Systems (IROS)*, pages 10843–10848. IEEE, 2020. 2
- [8] Hongbo Gao, Bo Cheng, Jianqiang Wang, Keqiang Li, Jianhui Zhao, and Deyi Li. Object classification using cnn-based fusion of vision and lidar in autonomous vehicle environment. *IEEE Transactions on Industrial Informatics*, 14(9):4224–4231, 2018. 2
- [9] Yushan Han, Hui Zhang, Huifang Li, Yi Jin, Congyan Lang, and Yidong Li. Collaborative perception in autonomous driving: Methods, datasets, and challenges. *IEEE Intelligent Transportation Systems Magazine*, 15(6):131–151, 2023. 1, 2
- [10] Yue Hu, Shaoheng Fang, Zixing Lei, Yiqi Zhong, and Siheng Chen. Where2comm: Communication-efficient collaborative perception via spatial confidence maps. *Advances in neural information processing systems*, 35:4874–4886, 2022. 2
- [11] Yue Hu, Yifan Lu, Runsheng Xu, Weidi Xie, Siheng Chen, and Yanfeng Wang. Collaboration helps camera overtake lidar in 3d detection. In *Proceedings of the IEEE/CVF Conference on Computer Vision and Pattern Recognition*, pages 9243–9252, 2023. 3
- [12] Sou Kitajima, Hanna Chouchane, Jacobo Antona-Makoshi, Nobuyuki Uchida, and Jun Tajima. A nationwide impact assessment of automated driving systems on traffic safety using multiagent traffic simulations. *IEEE Open Journal of Intelligent Transportation Systems*, 3:302–312, 2022. 1
- [13] Alex H Lang, Sourabh Vora, Holger Caesar, Lubing Zhou, Jiong Yang, and Oscar Beijbom. Pointpillars: Fast encoders for object detection from point clouds. In *Proceedings of the IEEE/CVF conference on computer vision and pattern recognition*, pages 12697–12705, 2019. 5
- [14] Jinlong Li, Baolu Li, Xinyu Liu, Runsheng Xu, Jiaqi Ma, and Hongkai Yu. Breaking data silos: Cross-domain learning for multi-agent perception from independent private sources. In *2024 IEEE International Conference on Robotics and Automation (ICRA)*, pages 18414–18420. IEEE, 2024. 1
- [15] Yiming Li, Shunli Ren, Pengxiang Wu, Siheng Chen, Chen Feng, and Wenjun Zhang. Learning distilled collaboration graph for multi-agent perception. *Advances in Neural Information Processing Systems*, 34:29541–29552, 2021. 3
- [16] Yiming Li, Juexiao Zhang, Dekun Ma, Yue Wang, and Chen Feng. Multi-robot scene completion: Towards task-agnostic collaborative perception. In *Conference on Robot Learning*, pages 2062–2072. PMLR, 2023. 3
- [17] Yen-Cheng Liu, Junjiao Tian, Nathaniel Glaser, and Zsolt Kira. When2com: Multi-agent perception via communication graph grouping. In *Proceedings of the IEEE/CVF Conference on computer vision and pattern recognition*, pages 4106–4115, 2020. 2
- [18] Yifan Lu, Quanhao Li, Baoan Liu, Mehrdad Dianati, Chen Feng, Siheng Chen, and Yanfeng Wang. Robust collaborative 3d object detection in presence of pose errors. In *2023 IEEE International Conference on Robotics and Automation (ICRA)*, pages 4812–4818. IEEE, 2023. 3
- [19] Yifan Lu, Yue Hu, Yiqi Zhong, Dequan Wang, Siheng Chen, and Yanfeng Wang. An extensible framework for open heterogeneous collaborative perception. In *The Twelfth International Conference on Learning Representations*, 2024. 1, 3, 5, 6
- [20] Tianyou Luo, Quan Yuan, Guiyang Luo, Yuchen Xia, Yujia Yang, and Jinglin Li. Plug and play: A representation enhanced domain adapter for collaborative perception. In *European Conference on Computer Vision*, pages 287–303. Springer, 2024. 1, 3
- [21] Congzhang Shao, Guiyang Luo, Quan Yuan, Yifu Chen, Yilin Liu, Kexin Gong, and Jinglin Li. Hetecooper: Feature collaboration graph for heterogeneous collaborative perception. In *European Conference on Computer Vision*, pages 162–178. Springer, 2024. 1
- [22] Steven E Shladover. Opportunities and challenges in cooperative road vehicle automation. *IEEE Open Journal of Intelligent Transportation Systems*, 2:216–224, 2021. 1
- [23] Sanbao Su, Yiming Li, Sihong He, Songyang Han, Chen Feng, Caiwen Ding, and Fei Miao. Uncertainty quantification of collaborative detection for self-driving. In *2023 IEEE International Conference on Robotics and Automation (ICRA)*, pages 5588–5594. IEEE, 2023. 2
- [24] Johan Thunberg, Galina Sidorenko, Katrin Sjöberg, and Alexey Vinel. Efficiently bounding the probabilities of vehi-

- cle collision at intelligent intersections. *IEEE Open Journal of Intelligent Transportation Systems*, 2:47–59, 2021. 1
- [25] Binglu Wang, Lei Zhang, Zhaozhong Wang, Yongqiang Zhao, and Tianfei Zhou. Core: Cooperative reconstruction for multi-agent perception. In *Proceedings of the IEEE/CVF International Conference on Computer Vision*, pages 8710–8720, 2023. 3
- [26] Tianhang Wang, Guang Chen, Kai Chen, Zhengfa Liu, Bo Zhang, Alois Knoll, and Changjun Jiang. Umc: A unified bandwidth-efficient and multi-resolution based collaborative perception framework. In *Proceedings of the IEEE/CVF International Conference on Computer Vision*, pages 8187–8196, 2023. 2
- [27] Tsun-Hsuan Wang, Sivabalan Manivasagam, Ming Liang, Bin Yang, Wenyuan Zeng, and Raquel Urtasun. V2vnet: Vehicle-to-vehicle communication for joint perception and prediction. In *Computer vision—ECCV 2020: 16th European conference, Glasgow, UK, August 23–28, 2020, proceedings, part II 16*, pages 605–621. Springer, 2020. 3
- [28] Xin Wang, Thomas E. Huang, Trevor Darrell, Joseph E Gonzalez, and Fisher Yu. Frustratingly simple few-shot object detection. 2020. 4
- [29] Sanghyun Woo, Jongchan Park, Joon-Young Lee, and In So Kweon. Cbam: Convolutional block attention module. In *Proceedings of the European conference on computer vision (ECCV)*, pages 3–19, 2018. 3
- [30] Hao Xiang, Runsheng Xu, and Jiaqi Ma. Hm-vit: Hetero-modal vehicle-to-vehicle cooperative perception with vision transformer. In *Proceedings of the IEEE/CVF international conference on computer vision*, pages 284–295, 2023. 3
- [31] Hua Xie, Yunjia Wang, Xieyang Su, Shengchun Wang, and Liang Wang. Safe driving model based on v2v vehicle communication. *IEEE Open Journal of Intelligent Transportation Systems*, 3:449–457, 2022. 1
- [32] Runsheng Xu, Yi Guo, Xu Han, Xin Xia, Hao Xiang, and Jiaqi Ma. Opennda: an open cooperative driving automation framework integrated with co-simulation. In *2021 IEEE International Intelligent Transportation Systems Conference (ITSC)*, pages 1155–1162. IEEE, 2021. 5
- [33] Runsheng Xu, Zhengzhong Tu, Hao Xiang, Wei Shao, Bolei Zhou, and Jiaqi Ma. Cobevt: Cooperative bird’s eye view semantic segmentation with sparse transformers. In *Conference on Robot Learning (CoRL)*, 2022. 3, 6
- [34] Runsheng Xu, Hao Xiang, Zhengzhong Tu, Xin Xia, Ming-Hsuan Yang, and Jiaqi Ma. V2x-vit: Vehicle-to-everything cooperative perception with vision transformer. In *European conference on computer vision*, pages 107–124. Springer, 2022. 3, 6
- [35] Runsheng Xu, Hao Xiang, Xin Xia, Xu Han, Jinlong Li, and Jiaqi Ma. Opv2v: An open benchmark dataset and fusion pipeline for perception with vehicle-to-vehicle communication. In *2022 International Conference on Robotics and Automation (ICRA)*, pages 2583–2589. IEEE, 2022. 3, 5, 6
- [36] Runsheng Xu, Jinlong Li, Xiaoyu Dong, Hongkai Yu, and Jiaqi Ma. Bridging the domain gap for multi-agent perception. In *2023 IEEE International Conference on Robotics and Automation (ICRA)*, pages 6035–6042. IEEE, 2023. 1, 3
- [37] Yan Yan, Yuxing Mao, and Bo Li. Second: Sparsely embedded convolutional detection. *Sensors*, 18(10):3337, 2018. 5
- [38] Kun Yang, Dingkan Yang, Jingyu Zhang, Mingcheng Li, Yang Liu, Jing Liu, Hanqi Wang, Peng Sun, and Liang Song. Spatio-temporal domain awareness for multi-agent collaborative perception. In *Proceedings of the IEEE/CVF international conference on computer vision*, pages 23383–23392, 2023. 3
- [39] Melih Yazgan, Thomas Graf, Min Liu, Tobias Fleck, and J Marius Zöllner. A survey on intermediate fusion methods for collaborative perception categorized by real world challenges. In *2024 IEEE Intelligent Vehicles Symposium (IV)*, pages 2226–2233. IEEE, 2024. 1
- [40] Syed Adnan Yusuf, Arshad Khan, and Riad Souissi. Vehicle-to-everything (v2x) in the autonomous vehicles domain—a technical review of communication, sensor, and ai technologies for road user safety. *Transportation Research Interdisciplinary Perspectives*, 23:100980, 2024. 1
- [41] Wenyuan Zeng, Shenlong Wang, Renjie Liao, Yun Chen, Bin Yang, and Raquel Urtasun. Dsdnet: Deep structured self-driving network. In *Computer Vision—ECCV 2020: 16th European Conference, Glasgow, UK, August 23–28, 2020, Proceedings, Part XXI 16*, pages 156–172. Springer, 2020. 2
- [42] Lihui Zhao and Andreas A Malikopoulos. Enhanced mobility with connectivity and automation: A review of shared autonomous vehicle systems. *IEEE Intelligent Transportation Systems Magazine*, 14(1):87–102, 2020. 1